

Heterogeneous Graph Contrastive Learning with Meta-path Contexts and Weighted Negative Samples

Jianxiang Yu*

Xiang Li *†

Abstract

Heterogeneous graph contrastive learning has received wide attention recently. Some existing methods use meta-paths, which are sequences of object types that capture semantic relationships between objects, to construct contrastive views. However, most of them ignore the rich meta-path context information that describes how two objects are connected by meta-paths. On the other hand, they fail to distinguish hard negatives from false negatives, which could adversely affect the model performance. To address the problems, we propose MEOW, a heterogeneous graph contrastive learning model that considers both meta-path contexts and weighted negative samples. Specifically, MEOW constructs a coarse view and a fine-grained view for contrast. The former reflects which objects are connected by meta-paths, while the latter uses meta-path contexts and characterizes the details on how the objects are connected. We take node embeddings in the coarse view as anchors, and construct positive and negative samples from the fine-grained view. Further, to distinguish hard negatives from false negatives, we learn weights of negative samples based on node clustering. We also use prototypical contrastive learning to pull close embeddings of nodes in the same cluster. Finally, we conduct extensive experiments to show the superiority of MEOW against other state-of-the-art methods.

1 Introduction

Heterogeneous information networks (HINs) are prevalent in the real world, such as social networks, citation networks, and knowledge graphs. In HINs, nodes (objects) are of different types to represent entities and edges (links) are also of multiple types to characterize various relations between entities. For example, in *Facebook*, we have entities like *users*, *posts*, *photos* and *groups*; users can *publish* posts, *upload* photos and *join* groups. Compared with homogeneous graphs where all the nodes and edges are of a single type, HINs contain richer semantics and more complicated structural information. To further enrich the information of HINs, nodes are usually associated with labels. Since ob-

ject labeling is costly, graph neural networks (GNNs) [16, 29, 4] have recently been applied for classifying nodes in HINs and have shown to achieve superior performance.

Despite the success, most existing heterogeneous graph neural network (HGNN) models require a large amount of training data, which is difficult to obtain. To address the problem, self-supervised learning, which is in essence unsupervised learning, has been applied in HINs [19, 10]. The core idea of self-supervised learning is to extract supervision from data itself and learn high-quality representations with strong generalizability for downstream tasks. In particular, contrastive learning, as one of the main self-supervised learning types, has recently received significant attention. Contrastive learning aims to construct positive and negative pairs for contrast, following the principle of maximizing the mutual information (MI) [17] between positive pairs while minimizing that between negative pairs. Although some graph contrastive learning methods for HINs have already been proposed [19, 11, 10], most of them suffer from the following two main challenges: *contrastive view construction* and *negative sample selection*.

On the one hand, to construct contrastive views, some methods utilize meta-paths [39, 30]. A meta-path, which is a sequence of object types, captures the semantic relation between objects in HINs. For example, if we denote the object types *User* and *Group* in Facebook as “U” and “G”, respectively, the meta-path *User-Group-User* (UGU) expresses the co-participation relation. Specifically, two users u_1 and u_2 are UGU-related if a path instance $u_1 - g - u_2$ exists, where g is a group object and describes the *contextual* information on how u_1 and u_2 are connected. The use of meta-paths can identify a set of path-based neighbors that are semantically related to a given object and provide different views for contrast. However, existing contrastive learning methods omit the contextual information in each meta-path view. For example, HeCo [30] takes meta-paths as views, but it only uses the fact that two objects are connected by meta-paths and discards the contexts of how they are semantically connected, which we will call *meta-path contexts* and can be very influential in

*East China Normal University. jianxiangyu@stu.ecnu.edu.cn, xiangli@dase.ecnu.edu.cn

†Corresponding author.

the classification task. For example, a group can provide valuable hints on a user’s topic interests. Therefore, contrasting meta-path views with rich contexts is a necessity.

On the other hand, negative sample selection is another challenge to be addressed. Note that most existing graph contrastive learning methods [33, 40, 5] are formulated in a sampled noise contrastive estimation framework. For each node in a view, random negative sampling from the rest of intra-view and inter-view nodes is widely adopted. However, this could introduce many *easy negative samples* and *false negative samples*. For easy negative samples, they are less informative and easily lead to the vanishing gradient problem [37], while the false negative samples can adversely affect the learning process for providing incorrect information. Recently, there exist some works [20, 37, 41] that seek to identify *hard negative samples* for improving the discriminative power of encoders in HINs. Despite their success, most of them fail to distinguish hard negatives from false ones. While ASA [20] is proposed to solve the issue, it is specially designed for the link prediction task and can only generate negative samples for objects based on one type of relation in HINs, which restricts its wide applicability. Since there is not a clear cut boundary between false negatives and hard ones, how to balance the exploitation of hard negative and false negative remains to be investigated.

In this paper, to solve the two challenges, we propose a heterogeneous graph contrastive learning method MEOw with meta-path contexts and weighted negative samples. Based on meta-paths, we construct two novel views for contrast: *the coarse view* and *the fine-grained view*. The coarse view expresses that two objects are connected by meta-paths, while the fine-grained view utilizes meta-path contexts and describes how they are connected. In the coarse view, we simply aggregate all the meta-paths and generate node embeddings that are taken as anchors. In the fine-grained view, we construct positive and negative samples for each anchor. Specifically, for each meta-path, we first generate nodes’ embeddings based on the meta-path induced graph. To further improve the generalizability of the model, we introduce noise by performing graph perturbations, such as *edge masking* and *feature masking*, on the meta-path induced graph to derive an augmented one, based on which we also generate node embeddings. In this way, each meta-path generates two embedding vectors for each node. After that, for each node, we fuse different embeddings from various meta-paths to generate its final embedding vector. Then for each anchor, its embedding vector in the fine-grained view is taken as a positive sample while those of other nodes are con-

sidered as negative samples. Moreover, to employ hard negatives and mitigate the adverse influence of false negatives, we learn the importance of negative samples. We perform node clustering and use the results to grade the weights of negative samples. To further boost the model performance, we employ prototypical contrastive learning [15], where the cluster centers, i.e., *prototype vectors*, are used as positive/negative samples. This helps learn compact embeddings for nodes in the same cluster by pushing nodes close to their corresponding prototype vectors and far away from other prototype vectors. Finally, we summarize our contributions as:

- We propose a novel heterogeneous graph contrastive learning model MEOw, which constructs a coarse view and a fine-grained view for contrast based on meta-paths, respectively. The former shows objects are connected by meta-paths, while the latter employs meta-path contexts and expresses how objects are connected by meta-paths.
- We distinguish hard negatives from false ones by performing node clustering and using the results to grade the weights of negative samples. Based on the clustering results, we also introduce prototypical contrastive learning to help learn compact embeddings of nodes in the same cluster.
- We conduct extensive experiments comparing MEOw with other 9 state-of-the-art methods w.r.t. node classification and node clustering tasks on three public HIN datasets. Our results show that MEOw achieves better performance than other competitors.

2 Related Work

2.1 Heterogeneous Graph Neural Network

Heterogeneous graph neural network (HGNN) has recently received much attention and there have been some models proposed. For example, HetGNN [35] aggregates information from neighbors of the same type with bi-directional LSTM to obtain type-level neighbor representations, and then fuses these neighbor representations with the attention mechanism. HGT [9] designs Transformer-like attention architecture to calculate mutual attention of different neighbors. HAN [29] employs both node-level and semantic-level attention mechanisms to learn the importance of neighbors under each meta-path and the importance of different meta-paths, respectively. Considering meta-path contexts information, MAGNN [4] improves HAN by employing a meta-path instance encoder to incorporate intermediate semantic nodes. Further, Graph Transformer Networks (GTNs) [32] are capable of generating new graph struc-

tures, which can identify useful connections between unconnected nodes in the original graph and learn effective node representation in the new graphs. Despite the success, most of these methods are semi-supervised, which heavily relies on labeled objects.

2.2 Graph Contrastive Learning (GCL)

Contrastive learning aims to construct positive and negative pairs for contrast, whose goal is to pull close positive pairs while pushing away negative ones. Recently, some works have applied contrastive learning to graphs [6, 42]. In particular, most of these approaches use data augmentation to construct contrastive views and adopt the following three main contrast mechanisms: (1) *node-node contrast* [21, 12, 27]; (2) *graph-graph contrast* [26, 33]; (3) *node-graph contrast* [7, 18]. For example, GRACE [40] treats two augmented graphs by node feature masking and edge removing as two contrastive views and then pulls the representation of the same nodes close while pushing the remaining nodes apart. Inspired by SimCLR [2] in the visual domain, GraphCL [31] further extends this idea to graph-structured data, which relies on node dropping and edge perturbation to generate two perturbed graphs and then maximizes the two graph-level mutual information (MI). Moreover, DGI [28] is the first approach to propose the contrast between node-level embeddings and graph-level embeddings, which allows graph encoders to learn local and global semantic information. In heterogeneous graphs, HeCo [30] takes two views from network schema and meta-paths to generate node representations and perform contrasts between nodes. HDGI [22] extends DGI to HINs and learns high-level node representations by maximizing MI between local and global representations. However, most of these methods select negative samples by random sampling, which will introduce false negatives. These samples will adversely affect the learning process, so we need to distinguish them from hard negatives.

2.3 Hard Negative Sampling

In contrastive learning, easy negative samples are easily distinguished from anchors, while hard negative ones are similar to anchors. Recent studies [23] have shown that contrastive learning can benefit from hard negatives, so there are some works that explore the construction of hard negatives. The most prominent method is based on mixup [36], a data augmentation strategy for creating convex linear combinations between samples. In the area of computer vision, Mochi [13] measures the distance between samples by inner product and randomly selects two samples from N nearest ones to be combined by mixup as synthetic negative sam-

ples. Further, CuCo [1] uses cosine similarity to measure the difference of nodes in homogeneous graphs. In heterogeneous graphs, STENCIL [41] uses meta-path-based Laplacian positional embeddings and personalized PageRank scores for modeling local structural patterns of the meta-path-induced view. However, these methods either fail to distinguish hard negative samples from false ones or are built on one type of relation in HINs, which restricts the wide applicability of these models.

3 Preliminary

DEFINITION 1. *Heterogeneous Information Network (HIN).* An HIN is defined as a graph $\mathcal{G} = (\mathcal{V}, \mathcal{E})$, where \mathcal{V} is a set of nodes and \mathcal{E} is a set of edges, each represents a binary relation between two nodes in \mathcal{V} . Further, \mathcal{G} is associated with two mappings: (1) node type mapping function $\phi : \mathcal{V} \rightarrow \mathcal{T}$ and (2) edge type mapping function $\psi : \mathcal{E} \rightarrow \mathcal{R}$, where \mathcal{T} and \mathcal{R} denote the sets of node and edge types, respectively. If $|\mathcal{T}| + |\mathcal{R}| > 2$, the network \mathcal{G} is an HIN; otherwise it is homogeneous.

DEFINITION 2. *Meta-path.* A meta-path $\mathcal{P}: T_1 \xrightarrow{R_1} T_2 \xrightarrow{R_2} \dots \xrightarrow{R_l} T_{l+1}$ (abbreviated as $T_1 T_2 \dots T_{l+1}$) expresses a composite relation $R = R_1 \circ R_2 \circ \dots \circ R_l$ between nodes of types T_1 and T_{l+1} , where \circ denotes the composition operator on relations. If two nodes x_i and x_j are related by the composite relation R , then there exists a path that connects x_i to x_j in \mathcal{G} , denoted by $p_{x_i \rightsquigarrow x_j}$. Moreover, the sequence of nodes and edges in $p_{x_i \rightsquigarrow x_j}$ matches the sequence of types T_1, \dots, T_{l+1} and relations R_1, \dots, R_l according to the node type mapping ϕ and the edge type mapping ψ , respectively. We say that $p_{x_i \rightsquigarrow x_j}$ is a path instance of \mathcal{P} , denoted by $p_{x_i \rightsquigarrow x_j} \vdash \mathcal{P}$.

DEFINITION 3. *Meta-path Context [16].* Given two objects x_i and x_j that are related by a meta-path \mathcal{P} , the meta-path context is the set of path instances of \mathcal{P} between x_i and x_j .

DEFINITION 4. *Heterogeneous Graph Contrastive Learning.* Given an HIN \mathcal{G} , our task is to learn node representations by constructing positive and negative pairs for contrast. In this paper, we only focus on one type of nodes, which are considered as target nodes.

4 Methodology

In this section, we introduce our method MEOW. The general model diagram is shown in Fig. 1. We perform feature transformation and neighbor filtering as preprocessing steps. First, we map the feature vectors of each different type of nodes into the same dimension (Step ①) and identify a set of neighbors for nodes

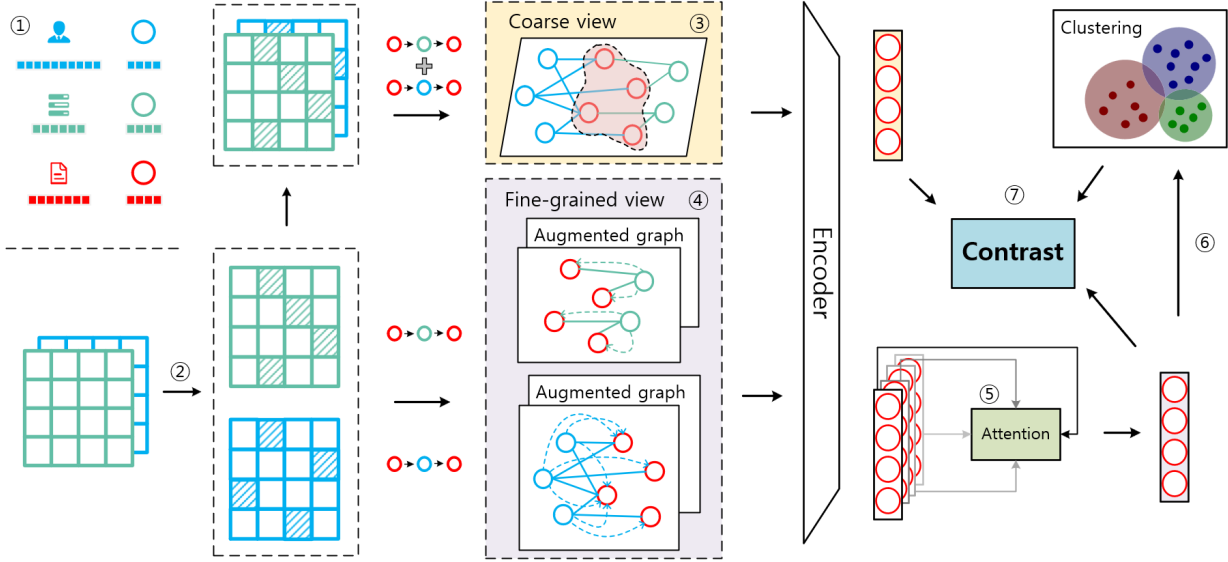


Figure 1: The overall framework of the MEOW model. For details of each step, see Section 4.

based on each meta-path (Step ②). Then, we construct a coarse view by aggregating all meta-paths (Step ③), while constructing a fine-grained view with each meta-path’s contextual semantic information (Step ④). After that, we fuse different embeddings from various meta-paths in the fine-grained view through the attention mechanism (Step ⑤). We take node embeddings in the coarse view as anchors and those in the fine-grained view as the positive and negative samples. To be capable of distinguishing false negative samples and hard negative samples, we perform clustering and assign weights to the negative samples with the clustering results (Step ⑥). Finally, to further boost the model performance, we use prototypical contrastive learning to calculate the contrastive loss and prototypical loss based on the node embedding vectors under coarse view and fine-grained view and the clustering results (Step ⑦). Next, we describe each component in detail.

4.1 Node Feature Transformation

Since an HIN is composed of different types of nodes and each type has its own feature space, we need to first preprocess node features to transform them into the same space. Specifically, for each object x_i in type T , we use the type-specific mapping matrix $W_T^{(1)}$ to transform the raw features of x_i into:

$$(4.1) \quad h_i = \sigma(W_T^{(1)} \cdot x_i + b_T),$$

where $h_i \in \mathbb{R}^d$ is the projected initial embedding vector of x_i , $\sigma(\cdot)$ is an activation function, and b_T denotes the bias vector.

4.2 Neighbor Filtering

Given an object x , meta-paths can be used to derive its multi-hop neighbors with specific semantics. When meta-paths are long, the number of related neighbors to x could be numerous. Directly aggregating information from these neighbors to generate x ’s embedding will be time-consuming. On the other hand, the irrelevant neighbors of x cannot provide useful information to predict x ’s label and they could adversely affect the quality of the generated embedding of x . Therefore, we filter x ’s meta-path induced neighbors and select the most relevant to x . Inspired by [16], we adopt *PathSim* [25] to measure the similarity between objects. Specifically, given a meta-path \mathcal{P} , the similarity between two objects x_i and x_j of the same type w.r.t. \mathcal{P} is computed by:

$$(4.2) \quad PS(x_i, x_j) = \frac{2 \times |\{p_{x_i \rightsquigarrow x_j} | p_{x_i \rightsquigarrow x_j} \vdash \mathcal{P}\}|}{|\{p_{x_i \rightsquigarrow x_i} | p_{x_i \rightsquigarrow x_i} \vdash \mathcal{P}\}| + |\{p_{x_j \rightsquigarrow x_j} | p_{x_j \rightsquigarrow x_j} \vdash \mathcal{P}\}|},$$

where $p_{x_i \rightsquigarrow x_j}$ is a path instance between x_i and x_j . Based on the similarities, for each object, we select its top- K neighbors with the largest similarity. The removal of irrelevant neighbors can significantly reduce the number of neighbors for each object, which further improves the model efficiency. After neighbor filtering, the induced adjacency matrix by meta-path \mathcal{P} is denoted as $A^{\mathcal{P}}$.

4.3 Coarse View

We next construct coarse view to describe which objects are connected by meta-paths. Given a set of

meta-paths, each meta-path \mathcal{P} can induce its own adjacency matrix $A^{\mathcal{P}}$. To provide a coarse view on the connectivity between objects by meta-paths, we fuse the meta-path induced adjacency matrices and define $\tilde{A} = \frac{1}{m}(A^{\mathcal{P}_1} + A^{\mathcal{P}_2} + \dots + A^{\mathcal{P}_m})$, where m is the number of meta-paths and $\tilde{A}^{\mathcal{P}_u} = D^{-1/2}A^{\mathcal{P}_u}D^{-1/2}$ is the normalized adjacency matrix. Here, D is a diagonal matrix with $D_{ii} = \sum_{j=1}^{|V|} A_{ij}^{\mathcal{P}_u}$, where $|V|$ is the number of target nodes. After that, we feed node embeddings calculated by Equation 4.1 and \tilde{A} into a two-layer GCN encoder to get the representations of nodes in the coarse view. Specifically, for node x_i , we can get its coarse representation z_i^c :

$$(4.3) \quad z_i^c = \text{Encoder}(\tilde{A}, h_i),$$

4.4 Fine-grained View

The fine-grained view characterizes how two objects are connected by meta-paths, which is in contrast with the coarse view. Given a meta-path set $\mathcal{PS} = \{\mathcal{P}_1, \dots, \mathcal{P}_m\}$, for each meta-path $\mathcal{P}_u \in \mathcal{PS}$, let $\mathcal{P}_u = T_0T_1\dots T_l$, where the meta-path length is $l + 1$. The meta-path can link objects of type T_0 to that of type T_l via a series of intermediate object types. Since meta-path contexts are composed of path instances and capture details on how two objects are connected, we utilize meta-path contexts to learn fine-grained representations for objects. However, when l is large, due to the numerous path instances between two objects, directly handling each path instance as MAGNN [4] could significantly degenerate the model efficiency, as pointed out in [16]. We instead use objects in the intermediate types of meta-path \mathcal{P}_u to leverage the information of meta-path contexts. Specifically, given a meta-path \mathcal{P}_u and an object x_i of type T_0 , we denote $N_i^{T_j}$ as x_i 's j -hop neighbor set w.r.t. \mathcal{P}_u . Then we generate x_i 's initial fine-grained embedding by aggregating information from all its j -hop neighbors with $j \leq l$. Formally, we have

$$(4.4) \quad h_i^{\mathcal{P}_u} = \sigma(h_i + \sum_{j=1}^l \sum_{x_v \in N_i^{T_j}} W_{uj}^{(2)} \cdot h_v),$$

where the learnable parameter matrix $W_{uj}^{(2)}$ corresponds to the j -hop neighbors w.r.t. \mathcal{P}_u . After that, we put the node embedding $h_i^{\mathcal{P}_u}$ that aggregates the meta-path context information and the adjacency matrix under the meta-path $\tilde{A}^{\mathcal{P}_u}$ into a two-layer GCN encoder to generate x_i 's fine-grained embedding:

$$(4.5) \quad z_i^{\mathcal{P}_u} = \text{Encoder}(\tilde{A}^{\mathcal{P}_u}, h_i^{\mathcal{P}_u}).$$

Note that the encoder here is the same as that used in the coarse view (see Equation 4.3). Further, to improve the model generalizability, we introduce noise to

the meta-path induced graph by performing graph augmentation, such as edge masking and feature masking. After the perturbed graph is generated, we feed it into Equation 4.5 to generate the node embedding $z_i^{\mathcal{P}_u}$. In this way, for each meta-path \mathcal{P}_u and an object x_i , we generate two embeddings $z_i^{\mathcal{P}_u}, z_i^{\tilde{\mathcal{P}}_u}$. Given a meta-path set $\mathcal{PS} = \{\mathcal{P}_1, \dots, \mathcal{P}_m\}$, we can generate $Z_i = \{z_i^{\mathcal{P}_u}, z_i^{\tilde{\mathcal{P}}_u} | \mathcal{P}_u \in \mathcal{PS}\}$ for node x_i from various meta-paths. Finally, we fuse these embeddings by the attention mechanism to generate x_i 's fine-grained embedding vector z_i^f :

$$(4.6) \quad z_i^f = \sum_{s=1}^{|Z_i|} \beta_s \cdot z_i^s, \quad \beta_s = \frac{\exp(w_s)}{\sum_{j=1}^{|Z_i|} \exp(w_j)},$$

where $w_s = \frac{1}{|V|} \sum_{x_i \in V} \mathbf{a}^T \cdot \tanh(W_{att}z_i^s + b_{att})$. Here, V is the set of target nodes, $W_{att} \in \mathbb{R}^{d \times d}$ is the weight matrix, b_{att} is the bias vector and β_s denotes the attention weight.

4.5 The MEOW model

After the coarse view and fine-grained view are constructed, we perform contrastive learning to learn node embeddings. Before contrast, we use a projection head to map node embedding vectors to the space where contrastive loss can be applied. Specifically, for x_i , we have:

$$(4.7) \quad \bar{z}_i^c = \sigma(W_{proj}z_i^c + b_{proj}), \quad \bar{z}_i^f = \sigma(W_{proj}z_i^f + b_{proj})$$

After that, we take representations in the coarse view as anchors and construct the positive and negative samples from the fine-grained view. For each node x_i , we take \bar{z}_i^c as the anchor, \bar{z}_i^f as the corresponding positive sample, and all other node representations in the fine-grained view as negative samples. Further, to utilize hard negatives and mitigate the adverse effect of false negatives, we learn the importance of negative samples. In particular, we perform node clustering based on the fine-grained representations for M times, where the number of clusters are set as $U = \{k_1, k_2, \dots, k_M\}$. Then, we assign different weights to negative samples of a node based on the clustering results. Intuitively, when the number of clusters is set large, each cluster will become compact. Then compared with hard negatives, false negatives and easy negatives are more likely to be assigned in the same cluster and different clusters with the anchor node, respectively. Therefore, we use γ_{ij} to denote the weight of node x_j as a negative sample to node x_i and set it as a function \mathcal{F} of clustering results. We denote $\gamma_{ij} = \mathcal{F}(C_1, C_2, \dots, C_M)$, where C_r is the r -th clustering result. In particular, we can understand γ_{ij} as the push strength. For false negatives, γ_{ij} should

Table 1: Quantitative results ($\% \pm \sigma$) on node classification.

Datasets	Metric	Split	GraphSAGE	GAE	Mp2vec	HERec	HetGNN	HAN	DGI	DMGI	HeCo	Ours
ACM	Ma-F1	20	47.13±4.7	62.72±3.1	51.91±0.9	55.13±1.5	72.11±0.9	85.66±2.1	79.27±3.8	87.86±0.2	88.56±0.8	91.93±0.3
		40	55.96±6.8	61.61±3.2	62.41±0.6	61.21±0.8	72.02±0.4	87.47±1.1	80.23±3.3	86.23±0.8	87.61±0.5	91.35±0.3
		60	56.59±5.7	61.67±2.9	61.13±0.4	64.35±0.8	74.33±0.6	88.41±1.1	80.03±3.3	87.97±0.4	89.04±0.5	92.10±0.3
	Mi-F1	20	49.72±5.5	68.02±1.9	53.13±0.9	57.47±1.5	71.89±1.1	85.11±2.2	79.63±3.5	87.60±0.8	88.13±0.8	91.82±0.3
		40	60.98±3.5	66.38±1.9	64.43±0.6	62.62±0.9	74.46±0.8	87.21±1.2	80.41±3.0	86.02±0.9	87.45±0.5	91.33±0.3
		60	60.72±4.3	65.71±2.2	62.72±0.3	65.15±0.9	76.08±0.7	88.10±1.2	80.15±3.2	87.82±0.5	88.71±0.5	91.99±0.3
	AUC	20	65.88±3.7	79.50±2.4	71.66±0.7	75.44±1.3	84.36±1.0	93.47±1.5	91.47±2.3	96.72±0.3	96.49±0.3	98.43±0.2
		40	71.06±5.2	79.14±2.5	80.48±0.4	79.84±0.5	85.01±0.6	94.84±0.9	91.52±2.3	96.35±0.3	96.40±0.4	97.94±0.1
		60	73.86±8.1	77.90±2.8	79.33±0.4	81.64±0.7	87.64±0.7	94.68±1.4	91.41±1.9	96.79±0.2	96.55±0.3	98.40±0.2
DBLP	Ma-F1	20	71.97±8.4	90.90±0.1	88.98±0.2	89.57±0.4	89.51±1.1	89.31±0.9	87.93±2.4	89.94±0.4	91.28±0.2	92.57±0.4
		40	73.69±8.4	89.60±0.3	88.68±0.2	89.73±0.4	88.61±0.8	88.87±1.0	88.62±0.6	89.25±0.4	90.34±0.3	91.47±0.2
		60	73.86±8.1	90.08±0.2	90.25±0.1	90.18±0.3	89.56±0.5	89.20±0.8	89.19±0.9	89.46±0.6	90.64±0.3	93.49±0.2
	Mi-F1	20	71.44±8.7	91.55±0.1	89.67±0.1	90.24±0.4	90.11±1.0	90.16±0.9	88.72±2.6	90.78±0.3	91.97±0.2	93.06±0.4
		40	73.61±8.6	90.00±0.3	89.14±0.2	90.15±0.4	89.03±0.7	89.47±0.9	89.22±0.5	89.92±0.4	90.76±0.3	91.77±0.2
		60	74.05±8.3	90.95±0.2	91.17±0.1	91.01±0.3	90.43±0.6	90.34±0.8	90.35±0.8	90.66±0.5	91.59±0.2	94.13±0.2
	AUC	20	90.59±4.3	98.15±0.1	97.69±0.0	98.21±0.2	97.96±0.4	98.07±0.6	96.99±1.4	97.75±0.3	98.32±0.1	99.09±0.1
		40	91.42±4.0	97.85±0.1	97.08±0.0	97.93±0.1	97.70±0.3	97.48±0.6	97.12±0.4	97.23±0.2	98.06±0.1	98.81±0.1
		60	91.73±3.8	98.37±0.1	98.00±0.0	98.49±0.1	97.97±0.2	97.96±0.5	97.76±0.5	97.72±0.4	98.59±0.1	99.41±0.0
AMiner	Ma-F1	20	42.46±2.5	60.22±2.0	54.78±0.5	58.32±1.1	50.06±0.9	56.07±3.2	51.61±3.2	59.50±2.1	71.38±1.1	71.09±0.3
		40	45.77±1.5	65.66±1.5	64.77±0.5	64.50±0.7	58.97±0.9	63.85±1.5	54.72±2.6	61.92±2.1	73.75±0.5	70.40±0.2
		60	44.91±2.0	63.74±1.6	60.65±0.3	65.53±0.7	57.34±1.4	62.02±1.2	55.45±2.4	61.15±2.5	75.80±1.8	72.82±0.5
	Mi-F1	20	49.68±3.1	65.78±2.9	60.82±0.4	63.64±1.1	61.49±2.5	68.86±4.6	62.39±3.9	63.93±3.3	78.81±1.3	78.03±0.2
		40	52.10±2.2	71.34±1.8	69.66±0.6	71.57±0.7	68.47±2.2	76.89±1.6	63.87±2.9	63.60±2.5	80.53±0.7	76.77±0.2
		60	51.36±2.2	67.70±1.9	63.92±0.5	69.76±0.8	65.61±2.2	74.73±1.4	63.10±3.0	62.51±2.6	82.46±1.4	78.88±0.3
	AUC	20	70.86±2.5	85.39±1.0	81.22±0.3	83.35±0.5	77.96±1.4	78.92±2.3	75.89±2.2	85.34±0.9	90.82±0.6	92.89±0.1
		40	74.44±1.3	88.29±1.0	88.82±0.2	88.70±0.4	83.14±1.6	80.72±2.1	77.86±2.1	88.02±1.3	92.11±0.6	92.88±0.1
		60	74.16±1.3	86.92±0.8	85.57±0.2	87.74±0.5	84.77±0.9	80.39±1.5	77.21±1.4	86.20±1.7	92.40±0.7	92.51±0.2

be small to ensure that they will not be pushed away from the anchor. For hard negatives, γ_{ij} is expected to be much larger because in this way, the anchor and hard negatives can be discriminated. Since easy samples are distant from the anchor, the model will be insensitive to γ_{ij} in a wide range of values. Then based on γ_{ij} , we can formulate our contrastive loss function as

$$(4.8) \quad \mathcal{L}_i^{con} = -\log \frac{\exp(\bar{z}_i^c \cdot \bar{z}_i^f / \tau)}{\sum_{j=1}^{|V|} \gamma_{ij} \exp(\bar{z}_i^c \cdot \bar{z}_j^f / \tau)}$$

where τ is a temperature parameter.

To further make embeddings of nodes in the same cluster more compactly distributed in the latent space, we introduce an additional prototypical contrastive learning loss function. In the r -th clustering, we consider the prototype vector c_i^r , i.e., the cluster center, corresponding to node x_i as a positive sample and other prototype vectors as negative samples and define:

$$(4.9) \quad \mathcal{L}_i^{proto} = -\frac{1}{M} \sum_{r=1}^M \log \frac{\exp(\bar{z}_i^c \cdot c_i^r / \theta_i^r)}{\sum_{j=1}^{k_r} \exp(\bar{z}_i^c \cdot c_j^r / \theta_j^r)}$$

where θ_i^r is a temperature parameter and represents the concentration estimate of the cluster C_r^i that contains node x_i . Following [15], we calculate $\theta_i^r = \frac{\sum_{q=1}^Q \|\bar{z}_q^c - c_i^r\|_2}{Q \log(Q + \alpha)}$, where Q is the number of nodes in the cluster and α is a smoothing parameter to ensure that small clusters do not have an overly-large θ . Finally, we

formulate our objective function \mathcal{L} as:

$$(4.10) \quad \mathcal{L} = \frac{1}{|V|} \sum_{x_i \in V} (\mathcal{L}_i^{con} + \lambda \mathcal{L}_i^{proto})$$

where V is the set of target nodes and λ controls the relative importance of the two terms. The loss function can be optimized by stochastic gradient descent. To prevent overfitting, we further regularize all the weight matrices W mentioned above.

5 Experiments

5.1 Datasets

To evaluate the performance of MEOw, we employ three real-world datasets: ACM [38], DBLP [4] and Aminer [8]. The three datasets are benchmark HINs. We next define a classification task for each dataset.

- **ACM:** The dataset contains 4019 papers (P), 7167 authors (A), and 60 subjects (S). Links include P-A (an author publishes a paper) and P-S (a paper is based on a subject). We use PAP and PSP as meta-paths. Paper features are the bag-of-words representation of keywords. Our task is to classify papers into three conferences: database, wireless communication, and data mining.
- **DBLP:** The dataset contains 4057 authors (A), 14328 papers (P), 20 conferences (C) and 7723 terms (T). Links include A-P (an author publishes a paper), P-T (a paper contains a term) and P-C (a

paper is published on a conference). We consider the meta-path set {APA, APCPA, APTPA}. Each author is described by a bag-of-words vector of their paper keywords. Our task is to classify authors into four research areas: Database, Data Mining, Artificial Intelligence and Information Retrieval.

- **AMiner**: The dataset contains 6564 papers (P), 13329 authors (A) and 35890 references (R). Links include P-A (an author publishes a paper) and P-R (a reference for a paper). We consider the meta-path set {PAP, PRP}. Our task is to classify papers into four research areas.

5.2 Baselines

We compare MEOW with 9 other state-of-the-art methods, which can be grouped into three categories:

- **[Methods specially designed for homogeneous graphs]**: GraphSAGE [6] aggregates information from a fixed number of neighbors to generate nodes’ embedding. GAE [14] is a generative method that generates representations by reconstructing the adjacency matrix. DGI [28] maximizes the agreement between node representations and a global summary vector.
- **[Semi-supervised learning methods in HINs]**: HAN [29] is proposed to learn node representations using node-level and semantic-level attention mechanisms.
- **[Unsupervised learning methods in HINs]**: HERec [24] utilizes the skip-gram model on each meta-path to embed induced graphs. HetGNN [34] aggregates information from different types of neighbors based on random walk with start. DMGI [18] constructs contrastive learning between the original network and a corrupted network on each meta-path and adds a consensus regularization to fuse node embeddings from different meta-paths. Mp2vec [3] generates nodes’ embedding vectors by performing meta-path-based random walks. Heco [30] constructs two views with meta-paths and network schema to perform contrastive learning across them. In particular, Heco is the state-of-the-art heterogeneous contrastive learning model.

5.3 Experimental Setup

We implement MEOW with PyTorch and adopt the Adam optimizer to train the model. We fine-tune the learning rate from {5e-4, 6e-4, 7e-4}, the penalty weight on the l_2 -norm regularizer from {0, 1e-4, 1e-3} and the patience for early stopping from 10 to 40 with step size 5, i.e., we stop training if the total loss does not decrease for patience consecutive epochs. We set the dropout rate ranging from 0.0 to 0.9, and the temperature τ in Eq. 4.8 from 0.1 to 1.0, both with step size 0.1. We set K in the neighbor filtering based on the average number of connections of all the objects under each

Table 2: Quantitative results (%) on node clustering.

Datasets	ACM		DBLP		AMiner	
	NMI	ARI	NMI	ARI	NMI	ARI
GraphSage	29.20	27.72	51.50	36.40	15.74	10.10
GAE	27.42	24.49	72.59	77.31	28.58	20.90
Mp2vec	48.43	34.65	73.55	77.70	30.80	25.26
HERec	47.54	35.67	70.21	73.99	27.82	20.16
HetGNN	41.53	34.81	69.79	75.34	21.46	26.60
DGI	51.73	41.16	59.23	61.85	22.06	15.93
DMGI	51.66	46.64	70.06	75.46	19.24	20.09
HeCo	56.87	56.94	74.51	80.17	32.26	28.64
Ours	66.21	71.17	75.46	81.19	33.91	33.81

meta-path. For data augmentation, we fine-tune the masking rate for both features and edges from 0.1 to 0.8 with step size 0.1. We perform node clustering twice and set $\alpha = 5$ in all datasets. Further, we set the number of clusters U to {100, 300}, {200, 700}, and {500, 1200} in ACM, DBLP, and Aminer, respectively. For simplicity, we calculate the negative sample weights $\gamma_{ij} = t$ based on the number of times t that the sample x_j and the anchor x_i are in different clusters. We fine-tune the regularization weights λ in prototypical contrastive learning from {0.1, 1, 10}. For Aminer, since nodes are not associated with features, we first run metapath2vec with the default parameter settings from the original codes provided by the authors to construct nodes’ initial feature vectors. For fair comparison, we set the embedding dimension as 64 and randomly run the experiments 10 times, and report the average results for all the methods. For other competitors, their results are directly reported from [30]. We provide our code and data here: <https://github.com/jianxiangyu/MEOW>.

5.4 Node Classification

We use the learned node embeddings to train a linear classifier to evaluate our model. We randomly choose 20, 40, 60 labeled nodes per class as training set, and 1000 nodes as validation set and 1000 nodes for testing. We use Macro-F1, Micro-F1 and AUC as evaluation metrics. For all the metrics, the larger the value, the better the model performance. The results are reported in Table 1. From the table, we see that MEOW achieves the best performance on ACM and DBLP, and performs very well on Aminer in all the data splits. This shows the importance of meta-path contextual information and the validity of the contrastive views we designed. Compared with the state-of-the-art graph contrastive learning model Heco, MEOW achieves better performance on ACM and DBLP. For example, the Macro-F1 score and the Micro-F1 score of Heco is 90.64% and 91.59% with 60 labeled nodes per class on DBLP, while the best score

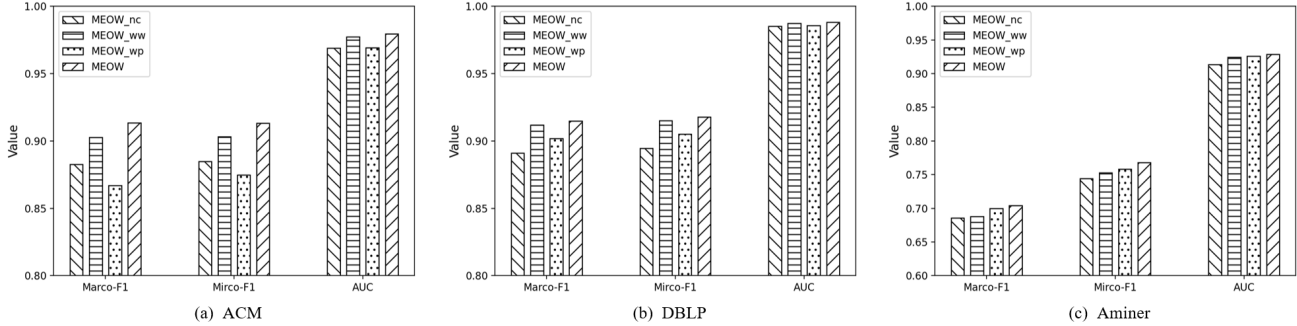


Figure 2: The ablation study results of 40 labeled nodes per class.

(MEOw) is 93.49% and 94.13%. These results show the effectiveness of MEOw. While MEOw performs slightly worse than Heco in Macro-F1 and Micro-F1 on Aminer, it outperforms Heco in the AUC scores. This can be explained by the label imbalance on Aminer. Specifically, the number of objects in the label which has the maximum number of nodes is ~ 7 times more than that in the label which has the minimum number of nodes. It is well known that when labeled objects are imbalanced, AUC is a more accurate metric than the other two. This further verifies that MEOw is effective.

5.5 Node Clustering

We further perform K-means clustering to verify the quality of learned node embeddings. We adopt normalized mutual information (NMI) and adjusted rand index (ARI) as the evaluation metrics. For both metrics, the larger, the better. The results are reported in Table 2. As we can see, MEOw outperforms all other methods significantly. In particular, on the ACM dataset, MEOw obtains about 16% improvements on NMI and 25% improvements on ARI over the runner-up method, demonstrating the superiority of our model. This is because the prototypical contrastive learning drives node representations to be more compact in the same cluster, which helps boost node clustering.

5.6 Ablation Study

We conduct an ablation study on MEOw to understand the characteristics of its main components. To show the importance of the prototypical contrastive learning regularization, we train the model with \mathcal{L}^{con} only and call this variant **MEOw_wp** (without **prototypical contrastive learning**). To demonstrate the importance of distinguishing hard negatives from false ones, another variant is to not learn the weights of negative samples. We call this **MEOw_w** (without **weight**). Moreover, we update nodes' embeddings by aggregating information without considering meta-path contexts in

the fine-grained view and call this variant **MEOw_nc** (**no context**). This helps us understand the importance of including meta-path contexts in heterogeneous graph contrastive learning. We report the results of 40 labeled nodes per class, which is shown in Fig.2. From these figures, MEOw achieves better performance than MEOw_wp. This is because the prototypical contrastive learning can drive nodes of the same label to be more compact in the latent space, which leads to better classification results. MEOw outperforms MEOw_w on three datasets. This further demonstrates the advantage of weighted negative samples. In addition, MEOw beats MEOw_nc in all cases. This shows that when using meta-paths, the inclusion of meta-path contexts is essential for effective heterogeneous graph contrastive learning.

6 Conclusion

We studied graph contrastive learning in HINs and proposed the MEOw model, which considers both meta-path contexts and weighted negative samples. Specifically, MEOw constructs a coarse view and a fine-grained view for contrast. In the coarse view, we took node embeddings derived by directly aggregating all the meta-paths as anchors, while in the fine-grained view, we utilized meta-path contexts and constructed positive and negative samples for anchors. To improve the model performance, we distinguished hard negatives from false ones by performing node clustering and using the results to assign weights to negative samples. Further, we introduced prototypical contrastive learning, which helps learn compact embeddings of nodes in the same cluster. Finally, we conducted extensive experiments to show the superiority of MEOw against other SOTA methods.

Acknowledgement

This work is supported by Shanghai Pujiang Talent Program No. 21PJ1402900, Shanghai Science and Tech-

nology Committee General Program No. 22ZR1419900 and National Natural Science Foundation of China No. 62202172.

References

- [1] F. CHE ET AL., *Multi-aspect self-supervised learning for heterogeneous information network*, Knowledge-Based Systems, 233 (2021), p. 107474.
- [2] T. CHEN ET AL., *A simple framework for contrastive learning of visual representations*, in ICML, PMLR, 2020, pp. 1597–1607.
- [3] Y. DONG ET AL., *metapath2vec: Scalable representation learning for heterogeneous networks*, in KDD, 2017, pp. 135–144.
- [4] X. FU ET AL., *Magnn: Metapath aggregated graph neural network for heterogeneous graph embedding*, in WebConf 2020, 2020, pp. 2331–2341.
- [5] H. HAFIDI ET AL., *Graphcl: Contrastive self-supervised learning of graph representations*, 2020.
- [6] W. HAMILTON ET AL., *Inductive representation learning on large graphs*, NeurIPS, 30 (2017).
- [7] K. HASSANI AND A. H. KHASAHMADI, *Contrastive multi-view representation learning on graphs*, in ICML, PMLR, 2020, pp. 4116–4126.
- [8] B. HU ET AL., *Adversarial learning on heterogeneous information networks*, in KDD, 2019, pp. 120–129.
- [9] Z. HU ET AL., *Heterogeneous graph transformer*, in WebConf, 2020, pp. 2704–2710.
- [10] D. HWANG ET AL., *Self-supervised auxiliary learning with meta-paths for heterogeneous graphs*, NeurIPS, 33 (2020), pp. 10294–10305.
- [11] X. JIANG ET AL., *Contrastive pre-training of gnns on heterogeneous graphs*, in CIKM, 2021, pp. 803–812.
- [12] N. JOVANOVIĆ ET AL., *Towards robust graph contrastive learning*, arXiv preprint arXiv:2102.13085, (2021).
- [13] Y. KALANTIDIS ET AL., *Hard negative mixing for contrastive learning*, NeurIPS, (2020), pp. 21798–21809.
- [14] T. N. KIPF AND M. WELLING, *Variational graph auto-encoders*, arXiv preprint arXiv:1611.07308, (2016).
- [15] J. LI ET AL., *Prototypical contrastive learning of unsupervised representations*, arXiv preprint arXiv:2005.04966, (2020).
- [16] X. LI ET AL., *Leveraging meta-path contexts for classification in heterogeneous information networks*, in ICDE, IEEE, 2021, pp. 912–923.
- [17] A. V. D. OORD ET AL., *Representation learning with contrastive predictive coding*, arXiv preprint arXiv:1807.03748, (2018).
- [18] C. PARK ET AL., *Unsupervised attributed multiplex network embedding*, in AAAI, 2020, pp. 5371–5378.
- [19] M. PARK, *Cross-view self-supervised learning on heterogeneous graph neural network via bootstrapping*, arXiv preprint arXiv:2201.03340, (2022).
- [20] X. QIN ET AL., *Relation-aware graph attention model with adaptive self-adversarial training*, in AAAI, vol. 35, 2021, pp. 9368–9376.
- [21] J. QIU ET AL., *Gcc: Graph contrastive coding for graph neural network pre-training*, in KDD, 2020, pp. 1150–1160.
- [22] Y. REN ET AL., *Heterogeneous deep graph infomax*, arXiv preprint arXiv:1911.08538, (2019).
- [23] J. ROBINSON ET AL., *Contrastive learning with hard negative samples*, arXiv preprint arXiv:2010.04592, (2020).
- [24] C. SHI ET AL., *Heterogeneous information network embedding for recommendation*, TKDE, 31 (2018), pp. 357–370.
- [25] Y. SUN ET AL., *Pathsim: Meta path-based top-k similarity search in heterogeneous information networks*, PVLDB, 4 (2011), pp. 992–1003.
- [26] S. SURESH ET AL., *Adversarial graph augmentation to improve graph contrastive learning*, NeurIPS, 34 (2021), pp. 15920–15933.
- [27] J. TANG ET AL., *Line: Large-scale information network embedding*, in WWW, 2015, pp. 1067–1077.
- [28] P. VELICKOVIC ET AL., *Deep graph infomax.*, ICLR (Poster), 2 (2019), p. 4.
- [29] X. WANG ET AL., *Heterogeneous graph attention network*, in WWW, 2019, pp. 2022–2032.
- [30] X. WANG, N. LIU, ET AL., *Self-supervised heterogeneous graph neural network with co-contrastive learning*, in KDD, 2021, pp. 1726–1736.
- [31] Y. YOU ET AL., *Graph contrastive learning with augmentations*, NeurIPS, 33 (2020), pp. 5812–5823.
- [32] S. YUN ET AL., *Graph transformer networks*, NeurIPS, 32 (2019).
- [33] J. ZENG AND P. XIE, *Contrastive self-supervised learning for graph classification*, in AAAI, vol. 35, 2021, pp. 10824–10832.
- [34] C. ZHANG ET AL., *Heterogeneous graph neural network*, in KDD, 2019, pp. 793–803.
- [35] C. ZHANG, D. SONG, ET AL., *Heterogeneous graph neural network*, in KDD, 2019, pp. 793–803.
- [36] H. ZHANG ET AL., *mixup: Beyond empirical risk minimization*, arXiv preprint arXiv:1710.09412, (2017).
- [37] Y. ZHANG ET AL., *Nscaching: simple and efficient negative sampling for knowledge graph embedding*, in ICDE, IEEE, 2019, pp. 614–625.
- [38] J. ZHAO ET AL., *Network schema preserving heterogeneous information network embedding*, in IJCAI, 2020.
- [39] J. ZHAO, Q. WEN, ET AL., *Multi-view self-supervised heterogeneous graph embedding*, in ECML-PKDD, Springer, 2021, pp. 319–334.
- [40] Y. ZHU ET AL., *Deep graph contrastive representation learning*, arXiv preprint arXiv:2006.04131, (2020).
- [41] Y. ZHU, Y. XU, H. CUI, C. YANG, Q. LIU, AND S. WU, *Structure-aware hard negative mining for heterogeneous graph contrastive learning*, arXiv preprint arXiv:2108.13886, (2021).
- [42] Y. ZHU, Y. XU, ET AL., *Graph contrastive learning with adaptive augmentation*, in WWW, 2021, pp. 2069–2080.